On Use of Independent Component Analysis for Ocular Artifacts Reduction of Electroencephalogram and while Using Kurtosis as the Threshold

Kazi Aminul Islam, Gleb Tcheslavski[*]

Department of Electrical Engineering
Lamar University
PO Box 10029, Beaumont, TX, 77710, USA
E-mails: russelkazi@yahoo.com, gleb@lamar.edu

[*]*Corresponding author*

Abstract: Brain electrical activity commonly represented by the Electroencephalogram (EEG), due to its miniscule amplitude (on the order of a hundred microvolts), is often contaminated with various artifacts. Independent Component Analysis (ICA) may be a useful technique to reduce some artifacts prior analyzing EEG. Present report discusses use of kurtosis to determine the threshold for detecting the artifacts-related independent components. Kurtosis may represent how peaked or how flat the artifacts that affect a signal are compared to the normal behavior of the original signal. Two statistical approaches were used for the kurtosis-based threshold selection: the Z-score and the confidence interval. The independent components determined as artifact-related may be either set to zero for the greater artifact suppression or scaled down for the reduced effect on the artifact-free regions of EEG. Based on the observed results, we may conclude that the present technique may be used for ocular artifacts reduction in EEG.

Keywords: Electroencephalogram, Independent Component Analysis (ICA), Kurtosis, Electro-ocular artifacts.

Introduction

Electroencephalogram (EEG) signals represent neural activities of the human brain. EEG is important for a number of medical applications including studies of epilepsy, trauma, and biofeedback. Due to its low amplitude (on the order of hundred microvolts), EEG is highly sensitive to various artifacts, such as ocular, cardiac, muscle, electrode, power-line noise, and external device artifacts. To extract the original neural signal, these artifacts should often be significantly minimized. The aim of this report is to consider, perhaps, the most damaging EEG artifacts – the electro-ocular artifacts (EOG) originating from the muscular activity of eyes.

The simplest and widely used method to minimize them is discarding the portions of EEG recording deemed as artifacts, based on exceeding a pre-determined threshold [8]. This approach, however, has its limitations. Apart from the uncertainties involved in the threshold selection, discharging portions of EEG dimmed as artifactual may also remove important neurological features. Another widely used method proposed by Gratton and colleagues relies on the existence of dedicated channels containing electrooculography data [6]. However, such dedicated EOG channels are not always available in practice, especially for consumer-grade EEG systems, such as EPOC by Emotiv. Alternatively, Independent Component Analysis (ICA) was utilized by Makeig, Bell, Jung, and Sejnowski to reduce EOG artifacts [11, 14]. The authors adopted the "infomax" algorithm for evaluation of independent

components in EEG analysis. The EEG data can be viewed as a set of signals at the electrode sites that are mixtures of neuro-related and artifactual components. Blind separation methods (BSS) reduce mixture of neural and non-neural variables to components, such that they are, in some way, independent of each other [10, 13]. Other than "infomax" techniques were utilized for ICA-based EEG analysis. This project utilizes one of such techniques, "fast ICA" introduced by Hyvärinen [7], for the independent components determination. However, most of ICA-based EOG minimizations rely on the existence of dedicated oculographic channels. Additionally, ICA by itself may not provide a method for selecting the independent components for elimination.

Joyce, Gorodnitsky, and Kutas [10] proposed a method where the artifactual components of EEG were identified manually for rejection. Javidi and Mandic [9] suggested identifying the artifactual component using the kurtosis value as a threshold. The purpose of this report is to explore two automatic procedures to identify and suppress the EOG artifacts of EEG, while not requiring EOG channels and utilizing the ICA.

Materials and methods

EEG acquisition and preprocessing

EEG data used in the project were acquired in the Applied DSP laboratory, Electrical Engineering department, Lamar University. Recordings were performed and pre-processed using Advanced Neuro Technology's (ANT, Netherlands) EEG acquisition system. A cap with 32 EEG electrodes positioned according to the International 10-20 System was used.

Due to their subtle amplitude, EEG data are often contaminated by different noise sources requiring preprocessing the signals first. DC offsets are often present in EEG. To minimize such an offset, a built-in MATLAB function 'detrend' was used. Spatial filtering is a technique minimizing surface currents in EEG that are produced by the neighboring channels. Common Average Reference (CAR) spatial filter for each electrode was applied. After that, Independent Component Analysis algorithm was implemented.

The aim of present report was to reduce EOG components in EEG. Eye-blink artifacts affect – to some extend – most of EEG channels. However, frontal channels are most influenced by EOG; therefore, the EEG recording for Fp_2 channel was selected for illustration.

Independent component analysis

ICA may perform somewhat better than other methods available for separating the independent components. In many practical uncorrelated situations, the signals would not be independent and are not easy to separate. The uncorrelated-ness itself would not be sufficient to screen out the artifacts. This is the reason that principal component analysis (PCA) may be not efficient for EEG artifacts separation. On the other hand, the ICA provides a method for artifacts removal where an accurate model of the process that generates the artifacts is not needed. Since the artifacts are usually independent from the rest of the signal, ICA is a promising technique for EEG artifact identification and removal [8].

Independent component analysis is a method that determines primary factors or components from the multivariate or multidimensional statistical data [8]. Let assume that the source signal $S_i(t)$ contains m variables and T observations. The observed signal $Y_i(t)$ is a linear combination of the source signal and a mixing matrix W [8]:

$$Y_i(t) = \sum_j W_{ij} S(t) \tag{1}$$

Un-mixing EEG data into components can be achieved through the following linear rotation [10]:

$$S = W^{-1} X . \tag{2}$$

Eq. (2) indicates that the EEG data X is rotated by the un-mixing matrix W^{-1} to produce the components of S. We observe that all quantities in (2) are matrices [10]. In this project, "fast ICA" MATLAB toolbox implementing the fast ICA algorithm [7] was used to estimate the independent components.

Kurtosis

The fourth order statistics – the kurtosis – is often employed in the ICA, while it may be used as a quantitative measure of the non-Gaussianity of random signals of the same type: either sub-Gaussian or super-Gaussian [8]. Kurtosis is defined as the standardized fourth central moment [5]:

$$k(x) = \frac{E\left\{(x-m)^4\right\}}{E\left\{(x-m)^2\right\}^2} = \frac{\mu_4}{\sigma^4} . \tag{3}$$

Here, $E\{*\}$ is the expectation operator, m is the mean, and σ is the standard deviation of data [5].

For the normal distribution, the process would have a kurtosis value of 3. That is why $k-3$ is often used, so that the reference normal distribution is described by a kurtosis of zero [5]. In the zero-mean case, definition of kurtosis may be simplified as [8]:

$$k(x) = E\left\{x^4\right\} - 3\left(E\left\{x^2\right\}\right)^2 . \tag{4}$$

The normalized kurtosis is defined as [8]:

$$\bar{k}(x) = \frac{E\left\{x^4\right\}}{\left(E\left\{x^2\right\}\right)^2} - 3. \tag{5}$$

The built-in MATLAB function "kurtosis" was used to estimate the kurtosis value for experimental data.

Z-scores

The standard deviation of a data set represents the dispersion of the samples around their mean. Assuming N samples, denoted as Y_n, with the mean M, the standard deviation can be evaluated as [1]:

$$S = \sqrt{\frac{\sum\limits_{n}(Y_n - M)^2}{N-1}} . \tag{6}$$

To normalize a set of data using the standard deviation, each data sample is divided by the standard deviation of the set. If the mean is subtracted from each sample prior this normalization, the result is known as Z-scores. Therefore, a set of N samples can be transformed into Z-scores as [1]:

$$Z_n = \frac{Y_n - M}{S} . \tag{7}$$

The set of Z-scores has a mean of zero and a standard deviation of one. Therefore, Z-scores constitute a unit-free measure that can be used to compare observations of different units [1, 12].

Confidence interval

The confidence interval is expressed by two numbers – the confidence limits – with the range in between that contains the values of the variable of interest with a certain level of confidence. The confidence level is often set to 95% indicating that "we may be 95% certain that the value is somewhere inside a 95% confidence interval" [2].

Assuming N observations, the confidence interval can be estimated as follows:

$$CI = \bar{x} \pm \frac{\sigma}{\sqrt{N}} t_{N-1} . \tag{8}$$

Here $N - 1$ is also the number of degrees of freedom. At 95% confidence level, the constant $t_{N-1} = 2.201$ for $N \leq 30$ and $t_{N-1} = 1.96$ for $N > 30$.

Artifactual component detection

ICA may separate EEG signals into the original source signals as independent components (ICs). After that, artifactual sources may be identified and removed. In semi-automatic and automatic artifact removal methodologies, several classifications (markers) based on the statistical characteristics of the ICs are considered allowing for the detection of artifacts in EEG. Next, these characteristics are compared against the threshold values to determine whether the particular components should be rejected. In these methods, the IC kurtosis has been utilized to identify and minimize those artifacts. Artifact-free EEG typically have a near-zero kurtosis value, which may indicate a Gaussian distribution. On the other hand, with artifacts, such as EOG, EEG exhibits a more peaked distribution with a highly positive kurtosis value. Using this kurtosis-based approach, we aim to extract artifacts as independent sources from the original EEG [9].

Two methods will be implemented to detect the threshold value for kurtosis.

Using Z-scores to determine the kurtosis threshold value

Kurtosis is positive for "peaked" sample distributions that may represent EOG artifacts, although it is negative for "flat" distributions that are typical for noise. For finding artifactual

ICs (outlier components), the EEG distributions are normalized with respect to all ICs to result in the distribution with zero-mean and unit standard deviation (Z-score). The decision threshold may be expressed as the multiple of the standard deviation and is usually selected as 1.64 [3]. If an IC exceeds the rejection threshold, it will be set to zero [3].

Using confidence interval to determine the kurtosis threshold value
The upper limit of the 95% confidence interval of the kurtosis of independent components will be used as the threshold. All the ICs with kurtosis exceeding the threshold are assumed to correspond to ocular artifacts and will be set to zero [4].

Results and discussion

Fig. 1 illustrates one second (256 samples) of EEG of the Fp_2 channel. DC offsets were eliminated by the built-in MATLAB 'detrend' function and the CAR spatial filter was applied.
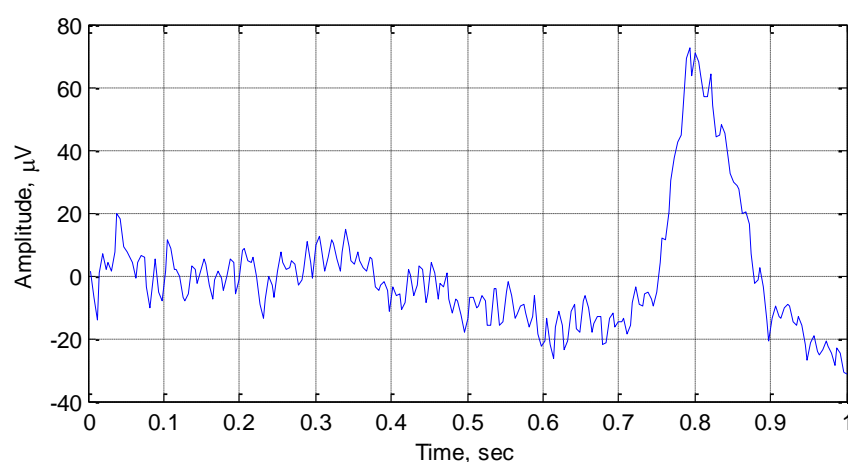
Fig. 1 A sample EEG fragment for Fp_2 channel containing an EOG artifact

The EEG channel Fp_2 was selected as one of the most affected by the ocular artifacts. The fragment depicted in Fig. 1 includes such an artifact from approximately 750 to 900 milliseconds.

Next, the ICs were evaluated by the "fast ICA" MATLAB toolbox resulting in 31 ICs. Fig. 2 illustrates the topographic maps of ICs estimated and plotted by EEGLAB.

Z-scores of kurtosis for the ICs were evaluated next for the sample EEG and are illustrated in Table 1. If the magnitude of Z-score of any IC exceeded 1.64 (selected as the threshold), this component was assumed as related to an ocular artifact and will be set to zero. The Z-scores exceeding the threshold are indicated by the red color in Table 1.

Alternatively, utilizing the confidence interval-based approach, the following quantities were evaluated for the kurtosis: sample mean = 7.672; sample standard deviation = 3.277; the confidence interval: 7.672 ± 1.153; upper confidence level (the threshold for the CI-based decision): 8.83. Therefore, the ICs, for which the kurtosis exceeds the threshold of 8.83, were assumed as related to artifacts, indicated by the red color in Table 1, and will be set to zero.
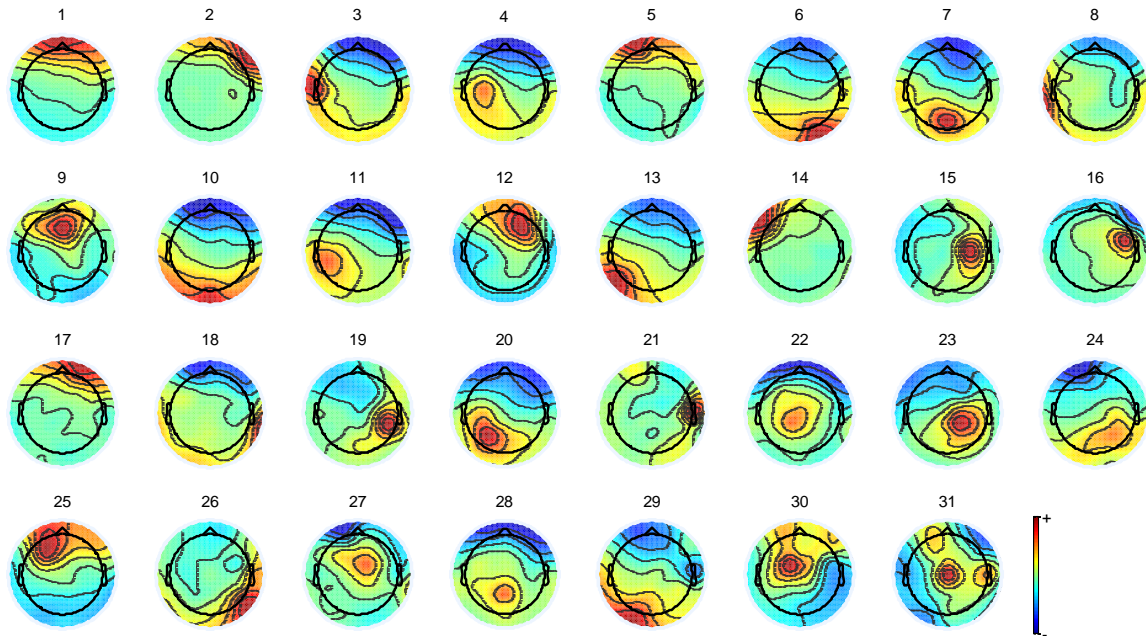
Fig. 2 Topographic maps of Independent Components evaluated for the sample EEG

Table 1. Z-scores of kurtosis and CI-based decisions
for different ICs evaluated for the sample EEG

IC number	1	2	3	4	5	6	7	8	9	10	
Kurtosis	10.4612	14.985	11.2541	16.097	9.0375	10.0066	8.6133	8.981	9.9804	12.1592	
Z-score	0.851	**2.231**	1.093	**2.571**	0.417	0.712	0.287	0.399	0.704	1.369	
CI-based	**yes**	**yes**	**yes**	**yes**	**yes**	**yes**	no	**yes**	**yes**	**yes**	
IC number	11	12	13	14	15	16	17	18	19	20	
Kurtosis	8.7642	8.8146	7.3491	6.6133	5.9161	6.8611	10.4211	8.8412	7.0169	5.5034	
Z-score	0.333	0.349	-0.099	-0.323	-0.536	-0.247	0.839	0.357	-0.1999	-0.662	
CI-based	no	no	no	no	no	no	**yes**	**yes**	no	no	
IC number	21	22	23	24	25	26	27	28	29	30	31
Kurtosis	5.7182	5.4632	6.7481	4.8235	4.6006	4.4669	4.601	3.848	4.2358	2.6864	2.9654
Z-score	-0.596	-0.674	-0.282	-0.869	-0.937	-0.978	-0.937	-1.167	-1.049	-1.521	-1.436
CI-based	no	no	no	no	no	no	no	no	no	no	no

We observe in Table 1 that the second and fourth ICs' Z-scores are 2.231 and 2.571. Since they exceed the threshold (of 1.64), we assume that these components predominantly represent EOG artifacts and, therefore, should be set to zero. On the other hand, using the confident interval-based approach, the components 1-6, 8-10, 17, and 18 have kurtosis exceeding the threshold (of 8.83) and are indicated for removal.

Fig. 3 illustrates the result of the artifact reduction using both methods: based on Z-score and on the confidence interval. The original EEG fragment is also shown as the reference.

We observe in Fig. 3 that both approaches lead to considerable reductions of the ocular artifact. On the other hand, we also observe that setting the ICs to zero affects the EEG signal outside the artifactual region, since the values of the signals before and after the artifact removal are

different, for instance, for the first 700 milliseconds of the fragment. Perhaps, the letter supports the conclusions of Castellanos and Makarov, who suggested that zeroing the ICs deemed artifactual may also affect neurological data [4]. Nevertheless, correlation coefficients evaluated between the original signal and the de-noised ones are 0.7335 and 0.5655 for the Z-score and CI-based methods, respectively. Therefore, we may conclude that the de-noised sequences are still somewhat related to the original signal (especially, when Z-scores were used).
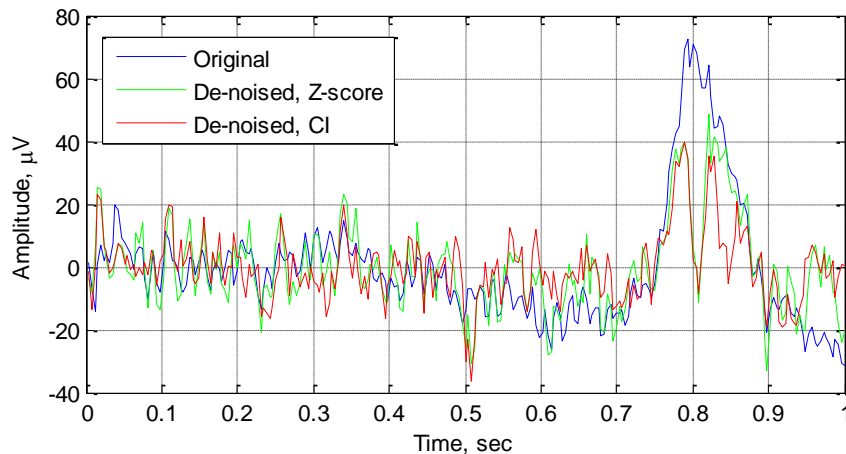
Fig. 3 A sample EEG fragment for Fp_2 channel
before and after EOG artifact reduction via ICs zeroing

Alternatively, the artifact itself may be of interest. Fig. 4 presents the reconstructed EOG artifact superimposed on the original EEG fragment. Both Z-score and CI can be used for the artifacts reconstruction. Unlike previously, (results in Fig. 2), only the independent components deemed as artifactual were maintained, while discarding everything else.
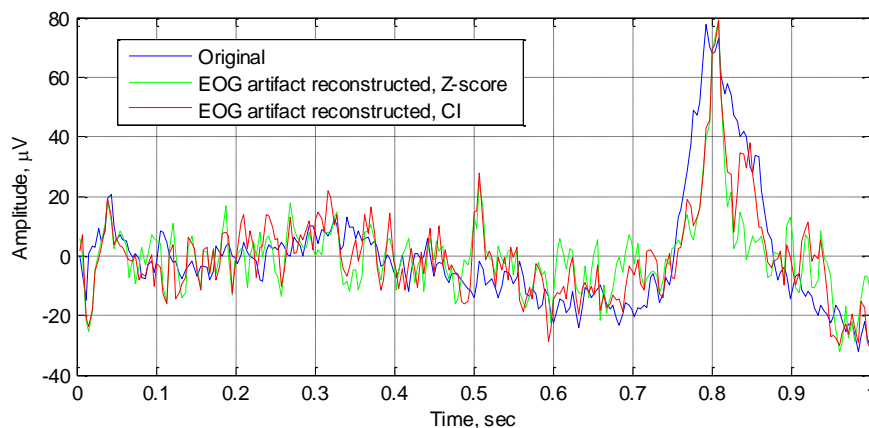
Fig. 4 A sample EEG fragment for Fp_2 channel
and the EOG artifact reconstructed via ICs zeroing

Comparing the reconstructed EOG with the original EEG signal, we observe that both the artifact position and its magnitude were evaluated correctly, although the artifact-free region (before approximately 0.7 s) appears somewhat noisier than in the original EEG.

To better understand the effects of artifact reduction, Power Spectral Density (PSD) estimates obtained via the Periodogram method are illustrated in Fig. 5 for the original EEG signal and

both de-noised versions. Before the analysis, the sequences were down-sampled by the factor 3 to eliminate high-frequency noise.
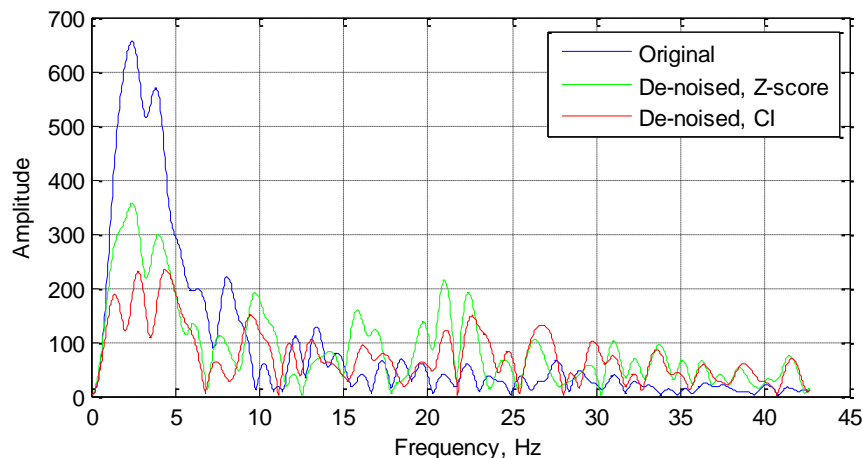
Fig. 5 Periodogram-based PSD estimates for a sample EEG fragment
of channel Fp_2 before and after EOG artifact reduction

We observe in Fig. 5 that the most pronounced effect of the artifact reduction may be seen in the low-frequency components of the sample sequence. Therefore, we may hypothesize that the eye blink predominantly manifested itself in the 2-4 Hz range. On the other hand, the component of the original EEG that was evident at approximately 8 Hz was shifted in frequency to 10 Hz. Additionally, the "de-noised" sequences exhibit considerable amount of power at 21-23 Hz, while the original EEG does not. Also, more power is evident in higher frequency components (exceeding 30 Hz) after artifact reduction. Bearing in mind the tendency of non-parametric spectral estimators to produce biased results for short data sequences, the effects seen in Figure 3 should be only considered as an illustration. Yet, we may suggest that zeroing independent components may lead to redistribution of spectral power of the sequences being processed.

As an alternative to zeroing, the independent components may be normalized, for instance, by the corresponding Z-scores. The results of such normalization are illustrated in Fig. 6 for the Z-score and CI-based techniques considered in this project.
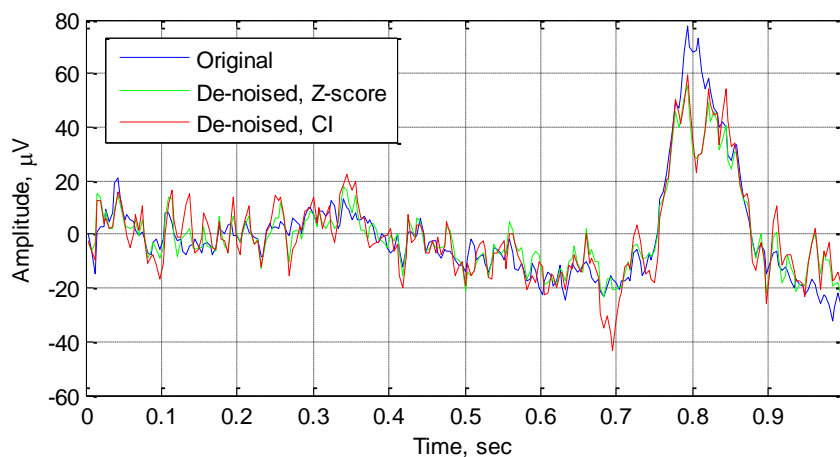
Fig. 6 A sample EEG fragment for Fp_2 channel
before and after EOG artifact reduction via ICs normalization

As seen in Fig. 6, normalization of Independent Components by the corresponding Z-score seems to produce less alteration in the artifact-free regions (up to 0.7 second time mark). The correlation coefficients evaluated between the original signal and the signals de-noised via the ICs normalization are 0.9329 and 0.8823 for the Z-score and CI-based methods, respectively. On the other hand, the ocular artifact suppression is less pronounced compared to the results depicted in Fig. 3 when the corresponding components were set to zero.

Conclusion

We discussed two robust and automated kurtosis-based methods of EEG artifactual components detection in conjunction with the Independent Components Analysis. Techniques based on both Z-score and confidence interval were capable for reducing ocular artifacts in EEG. On the other hand, zeroing independent components determined as artifact-related may also affect the artifact-free regions of EEG. However, scaling the corresponding independent components (instead of zeroing them) helps preserving the artifact-free portions of the original signal; although this approach diminishes the apparent artifact reduction capability.

This tradeoff between the artifact reduction performance and the need to preserve the artifact-free signal may be a factor limiting applications of ICA in artifacts minimization. On the other hand, EEG ocular artifacts are localized in time and, therefore, affect only relatively small portions of EEG recordings. Perhaps, applying the artifact reduction techniques only to the portions of the signal where artifacts are present may ease the above limitation. The latter may lead to a two-step artifact detection-minimization procedure, perhaps, applied with the variable-length time window.

Nevertheless, implementing Independent Component Analysis may be beneficial for the reduction of ocular artifacts in Electroencephalogram.

Acknowledgements

References

1. Abdi H. (2010). Normalizing Data: Encyclopedia of Research Design, In Salkind N. (Ed.), Thousand Oaks, CA: Sage.
2. Attia M. D. A. (2005). Why Should Researchers Report the Confidence Interval in Modern Research?, Middle East Fertility Society Journal, 10(1), 78-81.
3. Barbati G., C. Porcaro, F. Zappasodi, P. M. Rossini, F. Tecchio (2004). Optimization of an Independent Component Analysis Approach for Artifact Identification and Removal in Magneto-encephalographic Signals, Clinical Neurophysiology, 115(5), 1220-1232.
4. Castellanos N. P., V. A. Makarov (2006). Recovering EEG Brain Signals Artifact Suppression with Wavelet Enhanced Independent Component Analysis, Journal of Neuroscience Methods, 158, 300-312.
5. Decarlo L. T. (1997). On the Meaning and Use of Kurtosis, The American Psychological Association, Inc., 2(3), 292-307.
6. Gratton G., M. G. H. Coles, E. Donchin (1983). A New Method for Off-line Removal of Ocular Artifact, Electroencephalography and Clinical Neurophysiology, 55, 468-484.
7. Hyvärinen A. (1999). Fast and Robust Fixed-point Algorithms for Independent Component Analysis, IEEE Transactions on Neural Networks, 10(3), 626-634.
8. Hyvärinen A., J. Karhunen, E. Oja (2001). Independent Component Analysis, John Wiley & Sons, Inc.

9. Javidi S., D. P. Mandic (2010). Kurtosis Based Blind Source Extraction of Complex Noncircular Signals with Application in EEG Artifact Removal, Technical Report TR-ICU-BSE-1337/09-10. Updated 26 September, 2010.
10. Joyce C. A., I. F. Gorodnitsky, M. Kutas (2004). Automatic Removal of Eye Movement and Blink Artifacts from EEG Data Using Blind Component Separation, Psychophysiology, 41(2), 313-325.
11. Jung T.-P. S. Makeig, C. Humphries, T. W. Lee, M. J. McKeown, V. Iragui, T. J. Sejnowski (2000). Removing Electroencephalographic Artifacts by Blind Source Separation, Psychophysiology, 37, 167-178.
12. Khan M. S., S. Fazal (2015). Advanced Modelling and Functional Characterization of B2 Bradykinin Receptor, Int J Bioautomation, 19(2), 123-134.
13. Mahajan R., B. I. Morshed (2015). Unsupervised Eye Blink Artifact Denoising of EEG Data with Modified Multiscale Sample Entropy, Kurtosis, and Wavelet ICA, IEEE Journal of Biomedical and Health Informatics, 19(1), 158-165.
14. Makeig S., A. J. Bell, T.-P. Jung, T. J. Sejnowski (1996). Independent Component Analysis of Electroencephalographic Data, In Touretzky D., M. Mozer, M. Hasselmo (Eds.), Advances in Neural Information Processing Systems, Vol. 8, 145-151, Cambridge, MA, The MIT Press.

Kazi Aminul Islam, M.Sc.
E-mail: russelkazi@yahoo.com
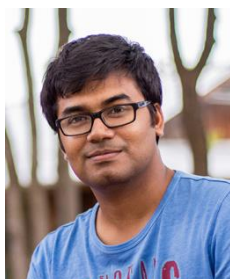
Kazi Aminul Islam has received his B.Sc. degree in Electrical and Electronic Engineering from Khulna University of Engineering and Technology. He also has completed his Masters in Electrical Engineering from Lamar University. His research interests are biomedical signal processing, image processing and machine learning.

Gleb V. Tcheslavski, Ph.D.
E-mail: gleb@lamar.edu

Gleb Tcheslavski has received his Engineer degree from Bauman Moscow State Technical University and Ph.D. in Electrical Engineering from Virginia Tech. Presently, he is with Drayer Department of Electrical Engineering, Lamar University.